17th World Conference on Earthquake Engineering, 17WCEE
Sendai, Japan - September 13th to 18th 2020

SEISMIC LIFE-CYCLE COST-BENEFIT ANALYSIS OF BRBs RETROFITTED FRAME

F. Freddi[(1)], J. Ghosh[(2)], M. Raghunandan[(3)], N. Kotoky[(4)]

[(1)]*Lecturer, University College of London, f.freddi@ucl.ac.uk*
[(2)]*Assistant Professor, Indian Institute of Technology Bombay, jghosh@iitb.ac.in*
[(3)]*Assistant Professor, Indian Institute of Technology Bombay, meerar@civil.iitb.ac.in*
[(4)]*Post-Doctoral Fellow, Indian Institute of Technology Bombay, needhi.iitg@gmail.com*

Abstract

Non-ductile buildings designed without consideration of modern seismic design principles may lead to damage, incurring loss of life and property following earthquake events. Alleviation of damage due to earthquakes is accomplished utilizing structural retrofitting techniques. Among the various viable retrofit measures, the use of buckling restrained braces (BRBs) has emerged to be promising, as indicated by past researchers. These braces provide a supplemental path for the earthquake-induced lateral loads and thus enhance the seismic behavior of the frame by adding energy dissipation capacity and, in some cases, stiffness to the bare frame. Consequently, this retrofitting technique leads to reduction in seismic losses in case of a future earthquake event. A frame can be designed for various retrofit level defined as the ratio between the base shear capacity of the bracing system and the bare frame. Since the infrastructure owners and stakeholders are often restricted by economic resources; it is crucial to estimate the cost-effectiveness of different retrofit level in terms of economic metrics by considering various sources of uncertainties into consideration.

A benchmark two-dimensional reinforced concrete frame with low ductility capacity is considered as a case study. The gravity load designed frame is retrofitted with BRBs for different retrofit level. The cost effectiveness of various retrofit level is conducted by a probabilistic approach where record-to-record variability of ground motions and BRB parameter uncertainty is considered to first develop seismic fragility curves of retrofitted frame for different retrofit level. Next, the fragility curves are used in conjunction with regional hazard information and repair costs data to evaluate the seismic life-cycle cost estimates of the retrofitted frame for various retrofit level. The study identifies the most viable retrofit level that result in minimum seismic life-cycle cost and consequently highest benefits in terms of retrofit implementation. The conclusions from this study aim to help infrastructure management agencies to assess investment decisions and identify the most cost-effective retrofit level for BRB design.

Keywords: Building frame; seismic retrofit; buckling restrained braces; seismic fragility curves; seismic life-cycle cost

17th World Conference on Earthquake Engineering, 17WCEE
Sendai, Japan - September 13th to 18th 2020

1. Introduction

In recent decades, seismic life-cycle cost analysis have emerged as an efficient and convenient tool for decision making towards channeling of limited monetary resources for retrofitting and rehabilitation of structures, especially when located in regions of moderate to high seismicity [1–4]. This methodology, in almost all of its forms and associated mathematical formulations utilizes information on building vulnerability under earthquakes, regional hazard information, and associated costs for building restoration to pre-hazard states[5,6]. As one would expect, a multitude of uncertainties exist in the seismic life-cycle cost estimation procedure. These sources of uncertainty may stem from the building parameters, modeling methodology, vulnerability analysis, hazard calculation, cost data, repair decisions, among others that invariably affect the seismic life-cycle cost [2]. For retrofitted structures, characteristics of the retrofit method adds an additional source of uncertainty that constitutes the main focus of this paper [7].

Among several of the modern retrofit strategies for older non-ductile moment resisting frame structures, the use of dissipative braces have emerged to be promising [8]. These dissipative braces function by providing a supplemental load path for the earthquake induced horizontal forces. Consequently, the seismic behavior of the bare frame is substantially enhanced through additional dissipation capacity and, in some cases, additional stiffness depending on the type of device [9]. This paper in particular investigates the effectiveness of Buckling Resistant Braces (BRBs) to reduce the seismic life-cycle cost in comparison to bare frame also systematically evaluates the influence of uncertainty in BRB parameters in loss assessment. These uncertainties typically stem from the manufacturing process and has also prompted international codes to set tolerances such that the BRB performance does not significantly deviate from the expected behavior [10–12]. The bare non-ductile moment resisting frame considered in this paper as a case-study example to test the effectiveness of BRBs in seismic vulnerability and life-cycle cost reductions is assumed to be located in Los Angeles, California. This frame is representative of the seismic design within the region prior to the advent of modern seismic design principles and also experimentally investigated by Bracci et al. 1992 [13], thereby providing opportinities for validation of the finite element model.

The paper is organized as follows: Section 2 provides a dicussion on the various sources of uncertainty in seismic vulnerability and loss predictions and outlines the scope of the present study. The subsequent section briefly details the seismic life-cycle cost estimation procedure adopted in this study to assess the lifetime losses and assess the influence of BRBs. Next, Section 4 presents details on the case-study frame, finite element modeling and validation with experimental results, as well as modeling of the BRB device aand associated uncertainties. Computations on seismic fragility of bare and retrofitted frame, fragility uncertainty bands and variations in seismic life-cycle costs are present next. The paper ends with conclusions and directions for future research in this area.

2. Sources of Uncertainty in Seismic Vulnerability and Economic Loss Predictions

Uncertainty quantification in seismic vulnerability and engineering loss estimation is of particular interest to building owners and stakeholders who are concerned about the risk posed by natural hazards [14]. Identifying the sources of uncertainty and quantifying their impact on the risk assessment of existing non-ductile buildings and when retrofitted with dissipative devices such as BRBs is essential to study the seismic resilience of these systems. This serves a two-fold purpose. Firstly, it helps assess the expected losses in older building stocks, and secondly it quantifies the benefits and the effectiveness of employing dissipative devices in reducing seismic vulnerability and seismic losses over a time horizon that spans through the service life of the structure. In addition to existing epistemic uncertainties occurring in nature and other “unknown-unknowns”, Table 1 lists a few sources of uncertainty which are known to influence direct loss estimates in buildings. Although evaluating all listed uncertainties is out of the scope of this paper, identifying the possible sources provides opportunities for future studies. This paper specifically focuses on the uncertainty stemming from ground motion record-to-record variability and BRB characteristics as further elaborated below.

Table 1: Example of known sources of uncertainty for seismic risk and economic direct loss of building structures.

Item	**Source of Uncertainty**
Hazard	Geophysics of faulting systems Ground motion prediction equations Ground motion record-to-record variability Hazard exceedance rates
Structure (Building)	Material properties Geometrical properties Deterioration parameters
Retrofit (BRB)	Device strength Device stiffness Strength proportion coefficient

The design properties for BRB devices are usually provided by the manufacturer and successively assessed by qualification control tests based on tolerance limits established by seismic and qualification codes [10–12]. For instance, the EN 15129 [12] requires to perform qualification tests to show the agreement with the nominal values for both the effective (*i.e.,* secant) stiffness $K_{eff,\,b}$ and effective damping $\xi_{eff,b}$. These two control parameters identify exhaustively the theoretical behavior of the device and therefore tolerance limits imposed on stiffness and damping parameters are also implicitly applied also to other related parameters, like forces and displacements [12]. Despite the nominal values of the properties of each device's type may be derived by experimental tests, the design codes allow device-to-device variations that may influence the seismic response. This variation reaches values of ±15% in the European codes and values up to ±20% in the American codes. This study assesses the impact of variation from design values on seismic fragility and life-cycle cost by considering uncertainty of the primary parameters affecting the BRB response, such as the device area (A_{BRB}) and the device material yield strength ($f_{y,BRB}$). To check the impact of variation on seismic fragility estimates, the lower and upper limits of the primary design parameters (A_{BRB}, $f_{y,BRB}$) are selected in such a way that the maximum force recorded in the braces does not deviate more than ±15% from the design value as per the tolerances defined in the acceptance criteria [12].

3. Seismic Life-Cycle Cost Assessment Methodology

As typical for seismic life-cycle cost (SLCC) evaluation, for the bare or the BRB-retrofitted frame, the critical inputs include the information on seismic vulnerability through fragility curves, regional seismic hazard data, and lastly the cost associated with the building damage. It is worthwhile to note that this study focuses only on probable lifetime seismic losses incurred as a consequence of repair following an earthquake damage and disregards costs stemming from other sources such as initial construction cost, building maintenance cost, among others. Developed either through a cloud analysis approach or incremental dynamic analysis, seismic fragility curves represent probabilistic statements on the likelihood of meeting or exceeding a particular damage state (or capacity limit state) given the intensity of ground motions. Mathematically, for a particular damage state *k* this may be represented as [15]:

$$P\left[D > C_k \,|\, IM = im\right] = \Phi\left[\frac{\ln(IM = im) - \ln(med)}{\beta}\right] \tag{1}$$

where, *D* represents the seismic demand imposed on the structure, C_k is the limit state capacity, *IM* represents the ground motion intensity measure with realization *im*, and *med* and β is the median and dispersion estimates of fragility. Next, seismic fragility curves are convolved with the region specific annual seismic hazard information $H(im)$ to evaluate the annual probability of exceeding the same damage state *k* as [16]:

$$PA_k = \int_{IM} P\left[D > C_k \left| IM = im \right.\right] \left| \frac{dH\left(im\right)}{d\left(im\right)} \right| d\left(im\right) \tag{2}$$

Assuming a homogeneous Poisson process of seismic events occurrence, and small exceedance probabilities typical for rare events such as earthquakes, the occurrence probabilities for being in a particular damage state *k* may be computed as:

$$\lambda_k = PA_{k,only} = PA_k - PA_{k+1} \tag{3}$$

Lastly, the yearly seismic losses across all damage states from $k = 1$ to K when aggregated over the service life of the structure, the expected seismic life-cycle cost can be evaluated as [17]:

$$E\left[SLCC\right] = \sum_{t=1}^{T} \sum_{k=1}^{K} \lambda_k e^{-\lambda_k t} \times \frac{C_k}{\left(1+\delta\right)^{t-1}} \tag{4}$$

where, T represents the service life of the bare or BRB-retrofitted frame, C_k is the cost of structural repair for a building in damage state k, and δ represents the inflation-adjusted discount rate.

The above procedure for seismic life cycle cost assessment as outlined from Equations (1) through (4) is conducted for the bare non-ductile frame as well for the retrofitted frame with different levels of uncertainty in the BRB design parameters. A comparison among the different cases help to estimate the expected reduction in lifetime SLCC as well the uncertainty in loss estimates one might expect stemming from the variability in BRB parameters alone. The next section of the paper introduces the modeling of bare frame, the BRB device, in addition to outlining the range of uncertainties expected in the BRB design parameters.

4. Case-study Building: Modeling of Bare and BRB-Retrofitted Frame

The case-study three-bay three-story non-ductile reinforced concrete (RC) moment-resisting frame (MRF) is shown in Fig. 1. For this case study frame, detailed experimental data may be found in past literature [13,18] that allows for validation of the numerical models at global and local level and thus serves as a benchmark for seismic fragility and life-cycle cost assessment. The height of each story within the frame is 3.66 m, while the width of the bay is 5.49 m. The building columns are square sections of 300 mm × 300 mm and beams are rectangular sections of 230 mm × 460 mm. The concrete compressive cube strength is employed as 24 MPa and the reinforcing bars as Grade 40 steel with a yield strength of 276 MPa. The building frame has been designed for gravity loads only without adequate seismic detailing as prevalent in buildings before the introduction of modern seismic codes. As also overlaid on the bare non-ductile frame, D-1 to D-3 in Fig. 1 indicates the placement of BRBs along the height of the frame in retrofitted frame. The present case study has been already numerically investigated by several authors [*e.g.*,[19,20]] and the following sections elaborate on the finite element modeling of the bare non-ductile frame and the BRB retrofitted frame.

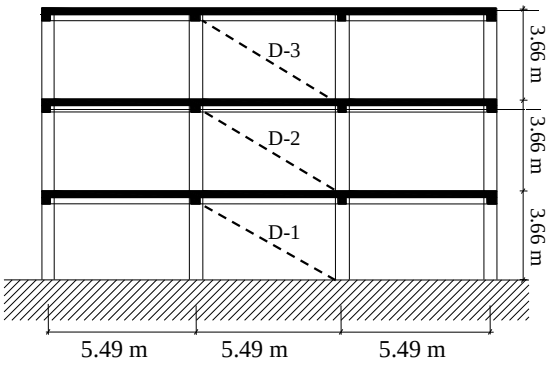

Fig. 1 Case-study bare frame (adapted from Bracci *et al.* [13]) and floor-wise layout of BRB device

4.1 Finite Element Modeling of Bare Non-Ductile Frame

This study utilizes the finite element package OpenSees [21] to develop a two-dimensional model of the structure. The beams and the columns of the frame are modeled using the *beamWithHinges* [22] element that comprises of linear elastic region in the central part and two fiber section at ends of the element to capture the plastic hinge behavior. The plastic hinge length within the beams and columns is defined following the recommendations of Panagiotakos and Fardis 2001[23]. The effective flexural stiffness of the elastic part is calculated using moment-curvature analysis of the section, considering the axial force level induced by dead loads. The ends of column and beams cross-section are defined using *FiberSection* with rectangular concrete patches and layers of reinforcement. Confined and unconfined concrete for the fiber sections, are modeled using the nonlinear degrading *Concrete02* material model. Longitudinal reinforcements are modeled using the *Hysteretic* material model whose parameters controlling pinching, damage and degraded unloading stiffness are calibrated using experimental results. In the beams, the contribution of the slab is modeled considering T-sections with effective width considered as 4 times the beam width. Since the columns of older non-ductile buildings may also be prone to shear failure, the shear response is simulated using a zerolength shear spring positioned at the column top. The characteristic properties of this shear spring are assigned using the *uniaxial limitstate* material developed by Elwood (2004) [24].

Building joints (exterior and interior) constitute critical locations where failure may be localized during seismic shaking. The joint model in this study includes a multi-linear response envelope and a tri-linear unload-reload path and is implemented using the *Pinching4* material [25] in OpenSees. The joint connection with the surrounding beams and columns is modeled using a two-node, zero-length rotational joint spring and four rigid offsets [20,26].The shear stress-strain response of the joints is simulated using a material model that defines joint moment versus rotation. As elaborated in Celik and Ellingwood (2008) [27], this moment-rotation relationship is determined from the joint shear stress-strain relationship using equilibrium and compatibility.

Subsequent to the elaborate modeling of the bare frame, similar to the work presented in [19,28] a validation of the proposed numerical model with experimental test results is necessary. In this regard, Bracci *et al.* 1995 [13] reports the results of the experimental tests carried on the 1:3 scale of benchmark frame. The results of snap back and white noise tests provide information about the frame vibration periods and the modal shapes. The first three natural periods measured in the experimental test results (0.537, 0.176 and 0.119 s) are in close agreement with the periods provided by the developed 1:3 scale finite model with uncracked gross stiffness properties (0.552, 0.172, and 0.100 s). A satisfactory agreement is also observed in the first three modal shapes. Furthermore, shake table tests results reported in Bracci *et al.* 1995 [13] provides additional opportunities for testing the adequacy of the proposed model. These tests include the time-history response data of the 1:3 scaled benchmark frame under the Kern County 1952, Taft Lincoln School Station, N021E component record scaled to different peak ground acceleration (PGA) levels of 0.05g, 0.20g and 0.30g. Fig. 2 shows the comparison of the top story displacements of the 1:3 scale experimental with 1:3 scale numerical model for the intensity level with PGA = 0.20g. The numerical result shows a satisfactory agreement with the experimental results for all the three intensities levels. Although not shown here, comparisons with experimental results of isolated columns and slab-beam-column subassemblages under cyclic loading also provide a satisfactory agreement thereby rendering confidence in the numerical model to predict the local element-level as well as the global response.

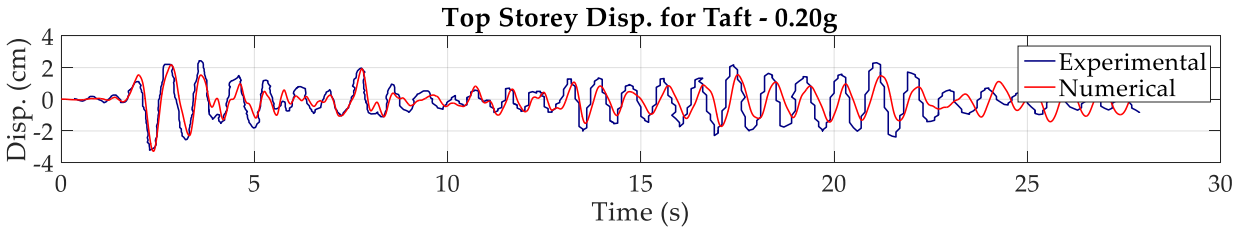

Fig. 2 Comparison of top displacements from the numerical model and experimental shaking table tests from Bracci *et al.* 1995 [13] when subjected to the scaled Taft ground motion with PGA = 0.20g

4.1 Modeling of BRB-Device, Retrofitted Frame, and Consideration of Uncertainties

4.1.1 BRB-Device modeling and placement within frame

For a realistic characterization of the fundamental hysteretic behavior of the BRBs, this study utilizes the *SteelBRB* material model [29] in OpenSees. This model captures the cyclic hardening and unequal tension and compression properties, unlike the idealized elastoplastic model traditionally used in literature [30]. As shown in Fig. 1, the brace with BRBs are placed in the central bay on each story (D1 to D3), thereby serving as a retrofit measure for the considered case-study frame. Each dissipative brace comprises of the elasto-plastic dissipative device (BRB) arranged in series with an elastic brace exhibiting adequate over-strength [31]. This arrangement conveniently allows the independent calibration of the stiffness (K_c^i) and strength (F_c^i) of the dissipative diagonal braces. The distribution of the stiffness K_c^i at each story is designed such that the first mode shape of the bare frame stays invariant upon placement of the retrofit [32,33]. This measure helps to avoid drastic changes to the internal action distribution in the frame, at least within the range of the elastic behavior. Additionally, the distribution of the strength F_c^i is typically designed to achieve the simultaneous yielding of the devices at all the stories such that the global ductility of the bracing system is the same as the ductility of the single braces. An extensive treatise on the nuances of the employed design strategy can be found in Dall'Asta *et al.* 2009 [32].

It is worthwhile to note that a frame can be designed/retrofitted for different values of the strength proportion coefficient (α) that defines the ratio between the base shear capacity of the bracing system and the bare frame, respectively. While this may contribute to yet another source of uncertainty, this study considers α = 1, leaving other estimates of this critical parameter and plausible uncertainties for future explorations. Another important parameter that controls the BRB design is the ductility of the dissipative brace (μ_{BRB}) that is assumed as 15 in this study following the recommendations of Uang and Nakashima 2004 [34]. In summary, Table 2 shows the properties of the dissipative braces K_c^i and F_c^i at each story together with the material's yield strength ($f_{y,BRB}$), the area (A_{BRB}) and length (L_{BRB}) of the BRB device.

Table 2 Design properties of the BRBs distributed across the floors of the retrofitted frame

Floor No.	F_c^i (kN)	K_c^i (kN/m)	$f_{y,BRB}$ (MPa)	A_{BRB} (mm^2)	L_{BRB} (mm)
1	207.9	45967.4	250.0	831.6	2799.3
2	178.9	30940.0	250.0	715.7	3579.2
3	103.0	28242.4	250.0	412.0	2257.4

4.1.2 Uncertainty within BRB design parameters

While the previous section and Table 2 enlists the BRB design parameters, the influence of these parameters uncertainties on seismic fragility and life-cycle cost needs to be evaluated. This study in particular considers uncertainty of the primary parameters affecting the BRB response, such as the device area (A_{BRB}) and the device material yield strength ($f_{y,BRB}$). To check the impact of variation on seismic fragility estimates, the lower and

upper limits of the primary design parameters (A_{BRB}, $f_{y,BRB}$) should be selected such that the maximum force recorded in the braces does not deviate more than ±15% from the design value as per the tolerances defined in the acceptance criteria [12]. Assuming that the device manufacturer uses the same material for the devices across all the three stories, the variation in $f_{y,BRB}$ can be neglected. Consequently, at present only the design area of device (A_{BRB}) at each story is considered as an uncertain parameter that affects both the strength (F_c^i) and stiffness (K_c^i) of the diagonal braces.

To assess the sensitivity of performance of retrofitted frame due to alteration in the design area of BRB device as compared to design parameters, a two-level full factorial design of experiment is employed. This experimental design strategy generates combinations of design parameters of the device at each floor by considering upper (+) and lower (-) extremities of parameter estimates. For the case at hand, these upper and lower estimates correspond to +15% and -15% from the design values of A_{BRB} respectively. Notwithstanding any correlation between the devices across different floors, Table 3 depicts the different combinations of the device area considered in this study.

Table 3: Two-level full factorial design generating different combinations of the device area A_{BRB} at different floors of the retrofitted case-study frame.

Combination	A_{BRB1}	A_{BRB2}	A_{BRB3}
1	+	+	+
2	-	-	+
3	+	-	-
4	+	-	+
5	-	+	+
6	+	+	-
7	-	-	-
8	-	+	+

5. Seismic Fragility and Life-Cycle Cost Analysis

This section of the paper focuses on seismic fragility and life-cycle cost assessment of the bare frame and retrofitted frames with BRB for a) design parameters, and b) uncertain parameters as listed in Table 3. First, details on the seismic fragility assessment are presented that includes elaborations on the ground motion selection, probabilistic seismic demand models and limit state capacities in terms of inter-story drift ratios. Next seismic fragility comparisons are carried out between the bare frame and retrofitted frame along with the "best" and "worst" BRB parameter combinations that leads to the least and the most fragile structure respectively. Subsequently seismic life-cycle cost computations underline the benefits of implementing BRBs for structural retrofitting and the expected uncertainties about the mean SLCC.

5.1 Seismic demand models and capacity estimates

Seismic demands models provide a one-to-one relationship between the ground motion intensity and an engineering demand parameter, that when used in conjunction with the capacity limit states helps establish seismic fragility curves. To develop such seismic demand models for the bare and retrofitted frames, this study utilizes a set of 150 unscaled ground motion records from the SIMBAD database [35] that provides a statistically significant number of strong-motion records of engineering relevance. The ground motion database includes shallow crustal earthquakes with moment magnitudes ranging from 5 to 7.3 and epicentral distances smaller than 35 km. Next, the analytical models for the case-study frames under consideration (bare or retrofitted) are subjected to this ground motion suite to develop the previously indicated one-to-one regression relationships as:

$$\ln(EDP) = r_1 + r_2 \ln(IM) + \varepsilon \tag{5}$$

where, *EDP* represents the engineering demand parameter considered to be maximum interstory drift ratio (IDR_{max}) in this study, r_1 and r_2 are the model regression coefficients, *IM* is the ground motion intensity measure (considered as spectral acceleration at the fundamental time period $Sa(T_1)$), and ε is the zero-mean error term that follows a Normal distribution and serves as a proxy for the lognormal standard deviation β_D for the seismic demand. Fig. 3(a) shows the comparison of the median of the demand models corresponding to the bare frame and the frame retrofitted with BRB with parameters at design values. This comparison underlines the reduction in seismic demand as a consequence of implementing the retrofit.

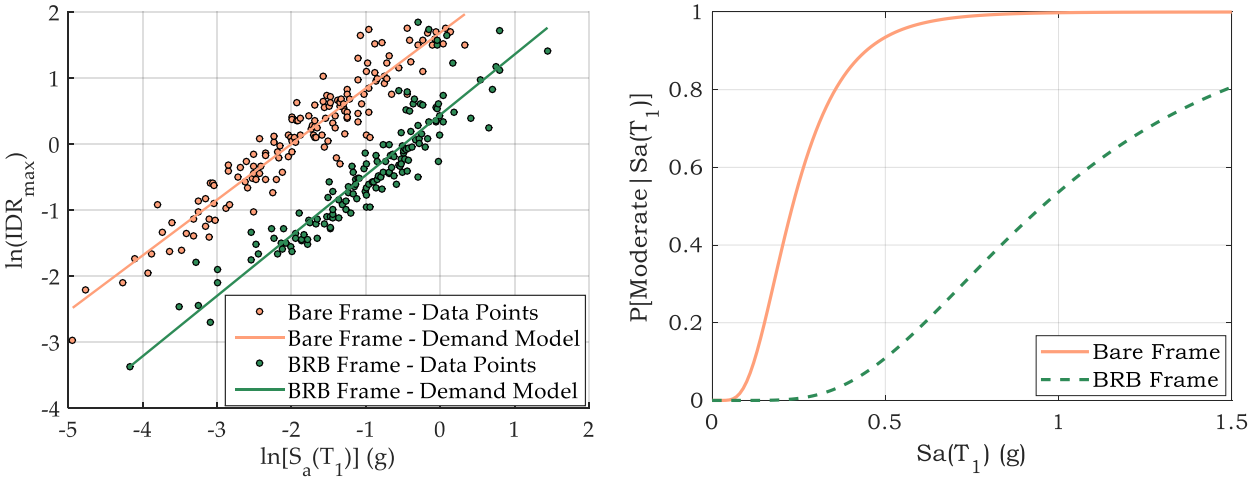

(a) (b)

Fig. 3 Comparison of (a) seismic demand models, and (b) seismic fragility curves (for moderate damage state) between the bare frame and retrofitted frame with design BRB parameters.

The limit state capacities for the bare frame as well as the retrofitted are obtained from non-linear static pushover analysis of the numerical model in OpenSees and tracking the response of the structure at each step. The discrete damage states in the building as: Slight, Moderate, Extensive and Complete, are identified based on the initiation of distinct physical behavior in the structure and quantified by the maximum IDR ratio (across all the stories) at which such behavior is observed. These physical behaviors associated with each of the defined damage states are reported in Table 2 along with the maximum inter-story drifts observed at the onset of each of the various damage states during the pushover analysis. It is worthwhile to note that for the BRB-retrofitted frame, pushover analysis along the two direction of the alignment of the BRBs results in two different value of IDRs as a consequence of altered compressive and tensile forces in frame members due to addition axial resistance provided by the BRBs. In the present study average value of the two IDRs are considered for the definition of the limit states for the retrofit frame. A dispersion β_C of 0.3 [36] is assumed in the definition of the capacity values in order to account for the uncertainty associated the definition of the damage states. Furthermore, for the BRB device itself, the damage state definitions are in terms of maximum ductility with limits as15 and 25 for extensive and complete damage states respectively.

Table 4. Damage states description & median IDR_{max} limits (S_C) for the bare frame and retrofitted frame with design BRB parameters

Damage States	Description	Maximum IDR (%)	
		Bare Frame	BRB Frame
Slight (S)	Yielding of 50% of columns at one floor	0.94	0.96
Moderate (M)	Crushing of concrete in 50 % of columns at one floor	1.50	1.50
Extensive (E)	Average of Moderate and Complete	2.71	2.76
Complete (C)	Initiation of shear failure in 50% of columns in one floor	3.90	4.00

Following the development of seismic demand regression relationships, a comparison with capacity estimates help estimate damage state specific seismic fragility curves as:

$$P\left[D > C \middle| Sa(T_1)\right] = \Phi\left[\frac{\ln\left\{Sa(T_1)\right\} - \frac{\ln(S_C) - r_1}{r_2}}{\frac{\sqrt{\beta_D^2 + \beta_C^2}}{r_2}}\right] \tag{6}$$

Above Equation (6) is in essence similar to fragility expression presented earlier in Equation (1) with the median of the fragility curve now computed as $med = \left[\ln(S_C) - r_1\right]/r_2$ and the lognormal standard deviation $\beta = \sqrt{\beta_D^2 + \beta_C^2}/r_2$. Fig. 4 (b) depicts a comparison of the seismic fragility between the bare frame and retrofitted frame with design BRB parameters for the moderate damage state highlighting the substantial reduction in building fragility. It is worthwhile to note that although the fundamental period of the bare and retrofitted frame differs, and such demand and fragility comparisons as presented in Fig. 3 should ideally be conducted for a structure-independent intensity measure, these representations still underline the influence of BRB retrofit towards reduction of seismic vulnerability. Moreover, the seismic life-cycle cost results presented later provides comparison on a more equitable platform.

5.2 Influence of BRB uncertainty on Seismic Fragility and Life-Cycle Costs

The previous section of the paper underlined the potential reduction of building fragility upon implementation of the BRB retrofit with design parameters. This section highlights the variation in fragility that may stem from the uncertainties of these design parameters as outlined earlier and subsequent impact on building life-cycle costs. In this regard, seismic fragility curves are first derived corresponding to each combination of the full factorial design presented in Table 3. It is worthwhile to note that the capacity limit states for each such

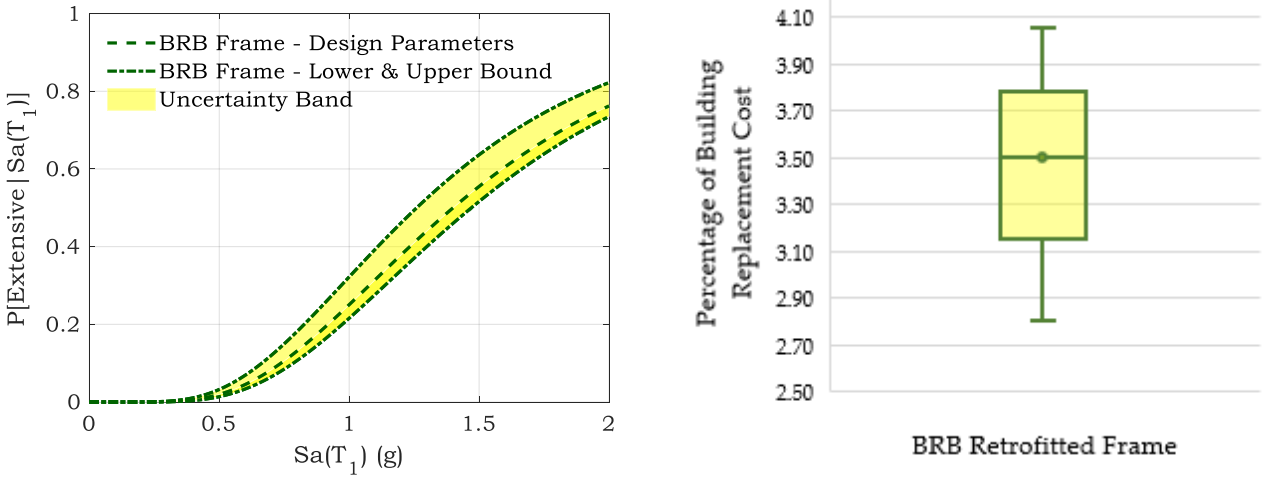

(a) (b)

Fig. 4 (a) Fragility curves and uncertainty bands considering design parameters and different combinations of the BRB design parameters listed in Table 3, and (b) variation of seismic life-cycle cost for the retrofitted frame as a percentage of building replacement cost.

combination obtained using pushover analysis remains similar to that for the frame with design BRB parameters (Table 4) and are hence kept unchanged for simplicity. Corresponding to the extensive damage state, Fig. 4(a) depicts the lower and upper bounds of the retrofitted frame fragility in addition to the fragility

for the design parameters. As expected, the lower bound corresponds to combination #1 from Table 3 wherein the area of the BRB devices are held at +15% at all floor levels generating the least fragile structure, and the upper bound corresponds to combination #7 with the area at least -15% estimates compared to the design parameters. Although not shown in the figure, the fragilities for other combinations fall in between the upper and lower bounds. Additionally, a separate Monte Carlo analysis revealed other uncertain parameter combinations result in fragilities fall within the bounds as depicted in Fig. 4(a)

The above fragilities are next used to compute the seismic life-cycle cost of the retrofitted frame in terms of percentage of the building replacement cost. A critical input required for fragility convolution and subsequent loss estimation constitutes the hazard information for the case study region. In this regard, the present study assumes the building to be located in Los Angeles, CA for which the hazard curve, $H(a)$ is obtained from USGS. Note that the Peak Ground Acceleration from the hazard curve data requires successive scaling by the spectrum in order to obtain the annual probability of exceeding specified levels of $S_a(T_1)$ for the case study bare frame and retrofitted structure. Additionally, the remaining service life is assumed as $T = 50$ years and the inflation-adjusted discount rate $\delta = 0.03$. The building repair cost ratios for different damage states are adopted from HAZUS and are assumed to be 0.4%, 1.9%, 9.6% and 19.2% of the building replacement cost.

Utilizing the above information and the mathematical framework outlined from Equations (1) through (4), seismic life-cycle costs as a percentage of building replacement costs are computed for the bare frame as well as the retrofitted frame corresponding to the design parameters and upper and lower fragility bounds. While for the bare frame, this percentage amounts to a substantial 109% of the replacement cost of the structure, for the retrofitted frame considering BRB uncertainties it ranges between 2.80% to 4.05% as shown in Fig. 4(b). These results clearly indicate the benefit of implementing BRB device for structural retrofit of older-designed non-ductile moment resisting frames as well as the appreciable uncertainty in seismic life-cycle costs stemming from the probably randomness within the BRB design parameters.

6. Conclusions

This paper focuses on assessing the sensitivity of BRB retrofit parameters on the seismic life cycle cost of bare and retrofitted non-seismically designed moment resisting frames. Seismic loss assessment along the lifetime of the structure requires knowledge on the structural characteristics, seismic vulnerability through fragility curves, information on regional seismic hazard, cost information, characteristics of the retrofit measure, among others. First, this study explores the different types of uncertainty that may stem from these sources with the aim to specifically explore the influence of randomness stemming from BRB retrofit on the life-cycle costs.

As a case-study structure this study chooses a three story – three bay RC frame (located in Los Angeles, California) corresponding to which experimental test data from past laboratory tests are available. The numerical model of the bare frame is first validated with the experimental tests before embarking on placing the retrofit to test BRB effectiveness in reducing vulnerability and seismic life-cycle cost. From the perspective of considering uncertainty in BRB parameters, this study chooses the area of the device that affects both the strength and stiffness of the braces. As per the recommendations in design codes regarding the tolerance levels, the device area is assumed to vary between +15% to -15% of the design estimates. Next, seismic fragility curves and life cycle costs derived for the bare and retrofitted frame (for design parameters as well as when considering uncertainty), reveals two critical observations. Firstly, implementation of the BRB device substantially reduces the seismic fragility and losses compared to the bare frame. For instance, seismic life-cycle cost for the bare unretrofitted frame amounts to approximately 109% of the building replacement cost, while for the design BRB parameters this amounts to only 3.5%. This underlines the effectiveness of BRB retrofit to reduce seismic vulnerability and economic losses during seismic shaking. Secondly uncertainty in the BRB parameters results in seismic losses that range between 2.8% to 4.1% of the replacement cost. While the latter upper bound, is almost 1.5 times the lower bound estimates in terms of percentage losses, one must note these losses derived in the present study correspond to structural components alone. Future studies on this

topic will also focus on non-structural components within the building to assess their contribution towards monetary losses in retrofitted building while considering uncertainties from various sources.

7. Acknowledgements

This research was funded by UGC-UKIERI joint research program (Grant No. 2017-UGC-10070). Any opinions, findings, and conclusions or recommendations expressed in this paper are those of the authors and do not necessarily reflect the views of the funding agencies.

8. References

1. Kappos AJ, Dimitrakopoulos EG. Feasibility of pre-earthquake strengthening of buildings based on cost-benefit and life-cycle cost analysis, with the aid of fragility curves. *Natural Hazards* 2008; **45**(1): 33–54.
2. Mitropoulou CC, Lagaros ND, Papadrakakis M. Life-cycle cost assessment of optimally designed reinforced concrete buildings under seismic actions. *Reliability Engineering & System Safety* 2011; **96**(10): 1311–1331.
3. Liu M, Burns SA, Wen YK. Optimal seismic design of steel frame buildings based on life cycle cost considerations. *Earthquake Engineering & Structural Dynamics* 2003; **32**(9): 1313–1332.
4. Chang SE, Shinozuka M. Life-cycle cost analysis with natural hazard risk. *Journal of Infrastructure Systems* 1996; **2**(3): 118–126.
5. Ghosh J, Padgett JE. Probabilistic seismic loss assessment of aging bridges using a component-level cost estimation approach. *Earthquake Engineering & Structural Dynamics* 2011; **40**(15): 1743–1761. DOI: 10.1002/eqe.1114.
6. Porter KA, Kiremidjian AS, LeGrue JS. Assembly-based vulnerability of buildings and its use in performance evaluation. *Earthquake Spectra* 2001; **17**(2): 291–312.
7. Kotoky N, Freddi F, Ghosh J, Raghunandan M. BRBs uncertainty propagation in seismic retrofit of RC structures. *13th International Conference on Applications of Statistics and Probability in Civil Engineering (ICASP13)*, Seoul National University; 2019.
8. Soong TT, Spencer Jr BF. Supplemental energy dissipation: state-of-the-art and state-of-the-practice. *Engineering Structures* 2002; **24**(3): 243–259.
9. Symans MD, Charney FA, Whittaker AS, Constantinou MC, Kircher CA, Johnson MW, *et al.* Energy dissipation systems for seismic applications: current practice and recent developments. *Journal of Structural Engineering* 2008; **134**(1): 3–21.
10. ASCE A. *Minimum design loads for buildings and other structures*. Reston, VA; 2010.
11. ASCE A. *Seismic Evaluation and Retrofit Rehabilitation of Existing Buildings*. Reston, VA; 2013.
12. EN C. 15129: Anti-seismic devices. *European Committee for Standardization, Bruxelles, Belgium* 2009.
13. Bracci JM, Reinhorn AM, Mander JB. Seismic resistance of reinforced concrete frame structures designed for gravity loads: performance of structural system. *Structural Journal* 1995; **92**(5): 597–609.
14. Tesfamariam S, Goda K. *Handbook of seismic risk analysis and management of civil infrastructure systems*. Elsevier; 2013.
15. Nielson BG, DesRoches R. Analytical Seismic Fragility Curves for Typical Bridges in the Central and Southeastern United States. *Earthquake Spectra* 2007; **23**(3): 615–633. DOI: 10.1193/1.2756815.

16. Padgett JE, Dennemann K, Ghosh J. Risk-based seismic life-cycle cost-benefit (LCC-B) analysis for bridge retrofit assessment. *Structural Safety* 2010; **32**(3): 165–173. DOI: 10.1016/j.strusafe.2009.10.003.
17. Nuti C, Vanzi I. To retrofit or not to retrofit? *Engineering Structures* 2003; **25**(6): 701–711. DOI: 10.1016/S0141-0296(02)00190-6.
18. Aycardi LE, Mander JB, Reinhorn AM. Seismic resistance of reinforced concrete frame structures designed only for gravity loads: experimental performance of subassemblages. *Structural Journal* 1994; **91**(5): 552–563.
19. Freddi F, Tubaldi E, Ragni L, Dall'Asta A. Probabilistic performance assessment of low-ductility reinforced concrete frames retrofitted with dissipative braces. *Earthquake Engineering & Structural Dynamics* 2013; **42**(7): 993–1011.
20. Jeon JS, Lowes LN, DesRoches R, Brilakis I. Fragility curves for non-ductile reinforced concrete frames that exhibit different component response mechanisms. *Engineering Structures* 2015; **85**: 127–143.
21. McKenna F, Fenves GL, Scott MH, Jeremic B. *Open System for Earthquake Engineering Simulation (OpenSees)*. Pacific Earthquake Engineering Research Center, University of California, Berkeley, CA: 2000.
22. Scott MH, Fenves GL. Plastic hinge integration methods for force-based beam–column elements. *Journal of Structural Engineering* 2006; **132**(2): 244–252.
23. Panagiotakos TB, Fardis MN. Deformations of reinforced concrete members at yielding and ultimate. *Structural Journal* 2001; **98**(2): 135–148.
24. Elwood KJ. Modelling failures in existing reinforced concrete columns. *Canadian Journal of Civil Engineering* 2004; **31**(5): 846–859.
25. Lowes LN, Mitra N, Altoontash A. A beam-column joint model for simulating the earthquake response of reinforced concrete frames 2003.
26. Alath S. Modeling inelastic shear deformation in reinforced concrete beam-column joints 1995.
27. Celik OC, Ellingwood BR. Modeling beam-column joints in fragility assessment of gravity load designed reinforced concrete frames. *Journal of Earthquake Engineering* 2008; **12**(3): 357–381.
28. Freddi F, Padgett JE, Dall'Asta A. Probabilistic seismic demand modeling of local level response parameters of an RC frame. *Bulletin of Earthquake Engineering* 2017; **15**(1): 1–23.
29. Gu Q, Zona A, Peng Y, Dall'Asta A. Effect of buckling-restrained brace model parameters on seismic structural response. *Journal of Constructional Steel Research* 2014; **98**: 100–113.
30. Fang C, Wang W. *Shape Memory Alloys for Seismic Resilience*. Springer; 2020.
31. Zona A, Dall'Asta A. Elastoplastic model for steel buckling-restrained braces. *Journal of Constructional Steel Research* 2012; **68**(1): 118–125.
32. Dall'Asta A, Ragni L, Tubaldi E, Freddi F. Design methods for existing rc frames equipped with elasto-plastic or viscoelastic dissipative braces, ANIDIS; 2009.
33. Ragni L, Zona A, Dall'Asta A. Analytical expressions for preliminary design of dissipative bracing systems in steel frames. *Journal of Constructional Steel Research* 2011; **67**(1): 102–113.
34. Uang CM, Nakashima M. Steel buckling-restrained braced frames. *Earthquake Engineering from Engineering Seismology to Performance-Based Engineering* 2004.
35. Smerzini C, Galasso C, Iervolino I, Paolucci R. Ground motion record selection based on broadband spectral compatibility. *Earthquake Spectra* 2014; **30**(4): 1427–1448.
36. FEMA. FEMA Library - HAZUS®MH MR4 Earthquake Model User Manual 2009. http://www.fema.gov/library/viewRecord.do?id=3732 [accessed March 12, 2011].

